ISBN 0140 3818
SSSU 39

AN AEROFOIL DESIGN METHOD FOR VISCOUS FLOWS

by C.J. Satchwell

July 1989

Ship Science Report No. 39

AN AEROFOIL DESIGN METHOD FOR VISCOUS FLOWS

By

C.J. Satchwell

Ship Science Report No. 39

June 1989

ABSTRACT

By convention, an aerofoil design problem involves finding the aerofoil shape corresponding to a prescribed surface velocity distribution. Various design methods have been devised for inviscid flows, including one based on an expression for the stream function on an aerofoil's surface. Present work extends this method to produce a matched viscous/inviscid iterative solution for the design of aerofoils in viscous flows.

Full derivations of new formulae are presented as well as a summary of essential formulae. Techniques for solving the underlying equations are examined, with particular emphasis on achieving a stable iteration. Comparisons are made between exact inviscid solutions for Karman–Treffetz aerofoils and viscous–flow solutions for aerofoils with the same surface velocity distributions. Results are plausible when displacement thickness effects are taken into account.

ACKNOWLEDGEMENT

The work described in this report was funded by the Commission of the European Communities as part of Contract EN3W.0016.UK (H1) between the Commission and the University of Southampton. Thanks are due to both the Commission and my colleagues in the Department of Ship Science, for financial and technical support, respectively.

NOMENCLATURE

a,b,c	(ξ,η) coordinates defined in Fig. A.1.2.
c	Chord
r	Leading edge radius
s,n	Local surface coordinates
x,y	Cartesian coordinates
u,v	Horizontal and vertical velocity components
w	Transpiration velocity through aerofoil surfaces
[A]	Influence coefficients for a panel method involving U(x) and γ
H	Shape factor (δ_1/θ)
L	Length scale to begin under-relaxation
N_1, N_2	Shape factors for vorticity variation (Fig. A.1.1)
R	Reynolds Number
U	Non-dimensional aerofoil surface velocity
Uo	Free stream velocity
α	Incidence
γ	Vorticity
δ_1	Displacement thickness
λ	Variable in Thwaite's method Eq. 32-34
θ	Angle of s axis to x axis (Geometrical context)
Θ	Momentum thickness (Boundary Layer context)
ψ	Stream function
ν	Kinematic viscosity
ω	Relaxation parameter
(ξ,η)	Local surface coordinates

Suffices

'	Dimensional variable
i	Collocation node (geometrical context)
i	Inviscid flow (viscous/inviscid matching context)
j	Vorticity node

n	Number of panels
w	Conditions at the wall

INTRODUCTION

Various authors have advanced methods for calculating the shape of an aerofoil corresponding to a prescribed surface velocity distribution for inviscid flows. Present work builds on previous work for inviscid flows, [refs (1) and (2)] to develop a similar method for viscous flows. The calculation of an aerofoil's shape from its surface velocity distribution is conventionally known as the aerofoil design problem. Of equal importance for real aerofoil design are the assessment of the characteristics required and the relationship between those characteristics and the aerofoil's surface velocity distribution. In the restricted jargon of aerodynamics, the two latter topics are not conventionally included in the 'design' problem and also lie outside the scope of the present paper.

The introduction of viscous effects into the design problem utilises ideas on matched viscous/inviscid solutions, where a real viscous flow (RVF) has its streamline–displacement effect computed and is then represented by an equivalent inviscid flow. A good account of this technique is described by Lock and Williams in ref (3). The main idea behind this technique is to achieve a smooth match with solutions for both the RVF and EIF. That idea is implicit in present work, i.e. it is a design method based on accurately–matched viscous and inviscid solutions. Another idea presented in ref (3) is that of a semi–inverse solution procedure where a direct (i.e. calculate U(x) knowing y(x)) inviscid solution is matched with an inverse (i.e. knowing w(x) calculate U(x)) boundary layer solution. In the present work, the considerable advantages of the semi–inverse algorithm are retained, but its implementation is reversed through the use of an inverse inviscid method and direct viscous method.

The starting point for the design problem is assumed to be a knowledge of the EIF velocity distribution either on an aerofoil, or on a displacement surface immediately proud of the aerofoil's surface. The solution procedure involves an iterative solution of a non–linear algebraic equation, derived from an expression for the stream function for the EIF on the aerofoil surface. Solution of this equation is achieved with the aid of two panel methods, both of which use linearly–varying vorticity elements with nodal collocation points. One of these involves a stream function/aerofoil shape relationship and the other a vorticity/velocity relationship. Various techniques are described to stabilise the solution process and derive a practical aerofoil design method for viscous flows.

Comparisons with inviscid Karman Treffetz aerofoil calculations are presented, as well as a sample calculation of an aerofoil derived from a more arbitrary surface velocity distribution.

OUTLINE OF THE DESIGN METHOD

The design method seeks to find an aerofoil shape corresponding to the equivalent inviscid flow (EIF) for some real viscous flow (RVF) around an aerofoil. Formulation of the inviscid problem follows classical stream function analysis e.g. Glauret, ref (4) but to avoid confusion, the notation of Soinne's report, ref (2) is adopted as present work builds that analysis.

Viscous flow calculations employ the methods of Heimenz, Thwaites, Smith, Gamberoni, ref (5) and Green, Weeks and Brooman, ref (6), for laminar boundary layer, transition and turbulent boundary layer calculations respectively. Results for displacement thickness (δ_1) are used to calculate surface stream function values for the required EIF and an inviscid analysis is then employed to estimate the aerofoil geometry.

FORMULATION OF THE INVISCID PROBLEM

Flow conditions are two dimensional, incompressible and irrotational. In these conditions, the stream function provides a measure of the volumetric flow across a boundary. In the case of an aerofoil without surface transpiration, the value of the stream function must be constant everywhere on the aerofoil surface since there is no flow through the surface. This stream function property can be used to solve classical problems of the surface velocity distribution corresponding to a given aerofoil shape (analysis problem) or the shape of an aerofoil corresponding to a given surface velocity distribution (design problem). The technique is to place vorticity panels over the aerofoil surface, relate vorticity strengths to the stream function value on the aerofoil and calculate either values of vorticity or the geometry of the aerofoil sought. Fig 1(a) shows this general arrangement with the notation in context and Fig 1(b) a detail of the panelised aerofoil.

The inviscid stream function model of ref (2) is summarised:

$$\frac{\partial \psi'}{\partial y'} = u \qquad (1)$$

$$\frac{\partial \psi'}{\partial x'} = -v \qquad (2)$$

Vorticity from elements δs of strength γ' are integrated over the aerofoil to produce a stream function of:

$$\psi' = \frac{1}{2\pi} \int_{\text{AEROFOIL}} \gamma'(s) \ln \left(\frac{r}{c}\right) ds \qquad (3)$$

Stream function changes associated with details of a position relative to the axis system are accounted for with the equation:

$$\psi'(x',y') = Uo\ (y' \cos\alpha - x' \sin\alpha) \qquad (4)$$

A stream function equation for a complete aerofoil can now be written:

$$\psi'_s = Uo\ (y' \cos\alpha - x' \sin\alpha) + \frac{1}{2\pi} \int_{\text{AEROFOIL}} \gamma'(s) \ln \left(\frac{r}{c}\right) ds \qquad (5)$$

A value of vorticity at some node 'j' will be collocated against a stream function value at point i such that equation (5) is re-written:

$$\psi' = U_o\ (y'_i \cos\alpha - x'_i \sin\alpha) - \sum_j k_{ij}\, \gamma'_j \qquad (6)$$

where K_{ij} is related to aerofoil geometry, the values of vorticity on panels adjacent to node j and the shape function chosen to represent vorticity variation (N_k) i.e.-

$$k_{ij} = \sum_k \frac{-1}{2\pi} \int_{\substack{\text{NODES} \\ \text{ADJACENT} \\ \text{TO j}}} N_k \ln \left(\frac{r}{c}\right) ds \qquad (7)$$

The problem is non-dimensionalised by dividing either with c or Uo.c. New variables lack the primes found in equations 1-7.

$$x = \frac{x'}{c} \tag{8}$$

$$y = \frac{y'}{c} \tag{9}$$

$$\gamma_j = \frac{\gamma_j'}{Uo\ c} \tag{10}$$

$$\psi = \frac{\psi'}{Uo\ c} \tag{11}$$

Using the new variables, equation (6) becomes:

$$\psi = yi\ \cos\alpha - xi\ \sin\alpha - \sum_j k_{ij}\ \gamma_j \tag{12}$$

Equation (12) provides the basis for an analysis method whereas for a design method the equation is re-arranged to provide an estimate of y_i as:

$$yi = \frac{1}{\cos\alpha}\ \left[\psi + x_i\ \sin\alpha + \sum_j k_{ij}\ \gamma_j\right] \tag{13}$$

Equation (13) or its equivalent is a well-known Fredholms integral equation of the first kind, to which many solutions have been offered e.g. ref's (1) and (2). Present work is concerned with stabilising the solution process and the inclusion of viscous effects; through the calculation of an appropriate transpiration velocity to represent displacement effects of the boundary layer.

EXTENSIONS TO INCLUDE VISCOUS EFFECTS

The growth of a boundary layer over a surface has a displacement effect on external-flow streamlines equivalent to moving the surface outwards by an amount δ_1. Following the notation of ref (3), where suffix i is used to denote inviscid conditions and suffix w the conditions at the wall, a transpiration velocity $(-\partial\psi/\partial s)$ for the EIF can be found from continuity considerations as:

$$- \frac{\partial \psi'}{\partial s} \cdot \delta s = \int_o^{\delta} \frac{\partial}{\partial s} (U_i - U) \, dn \qquad (13)$$

$$= \frac{d}{ds} \int_o^{\delta} (U_i - U) \, dn \qquad (14)$$

defining δ_1, as $$\frac{1}{U_{iw}} \int_o^{\delta} (U_i - U) \, dn \qquad (15)$$

then $$- \frac{\partial \psi'}{\partial s} \cdot \delta s = \frac{d}{ds} (U_{iw} \, \delta_1) \qquad (16)$$

Integrating from a stagnation point along the surface (where n=0) leads to the equation

$$\psi' = \text{constant} - U_{iw} \, \delta_1 \qquad (17)$$

At a stagnation point, U_{iw} is zero and the stream function is denoted by ψs.

Consequently,

$$\psi' = \psi'_s - U_{iw} \, \delta_1(s) \qquad (18)$$

Equation (18) provides a basis for including viscous effects into the stream function design method. Instead of using a constant value of ψ' (appropriate to an inviscid flow problem) it is possible to vary the values of ψ' along the surface of the aerofoil to reflect the growth in displacement thickness, as indicated by equation (18). In practice, the choice of a starting value of ψ_s' simply determines the position of the aerofoil on the y axis but not the shape of the resulting section. it is therefore possible to simplify equation (19) by taking $\psi s'$ as zero, revert back to the notation that i corresponds to a collocation point and write:

$$\psi_i' = U_i \, \delta_{ij} \qquad (19)$$

Non-dimensionalising leads to:

$$\psi_i = - \frac{U_i}{U_o} \frac{\delta 1 i}{c} \qquad (20)$$

Equation (13) is now modified to introduce viscous effects as:

$$y_i = \frac{1}{\cos\alpha} \left[\psi_i + x_i \sin\alpha + \sum_j k_{ij} \gamma_j \right] \qquad (21)$$

where the values of ψ_i come from equation (20).

Equation (21) can be solved directly for an appropriate surface velocity distribution, but fails to converge for velocity distributions that are not feasible. More will be said on this topic later.

STRATEGIC CONSIDERATIONS FOR A SOLUTION

Equation (21) is an algebraic equation derived from a Fredholms integral equation of the first kind, for which a solution cannot be guaranteed. previous authors, refs (1) and (2) have commented on problems of numerical stability in solutions to equation (13). The problem is that equation (13) needs to be solved iteratively - starting with an initial estimate of aerofoil geometry and a chordwise velocity distribution, computing values for γ_j and finally estimating y_i to provide the next iteration for aerofoil geometry. There is no guarantee that this iterative procedure will always be stable, especially when starting from an arbitrary initial estimate of aerofoil geometry. Any errors in relating γ_j to u_i will probably magnify instabilities. Equation (21) is potentially less stable than (13), as it makes provision for displacement effects of viscous flow to be included.

With all these uncertainties, as well as a degree of vagueness in the literature about previous efforts to relate γ_j to u_i, a solution strategy had to be devised. Initial considerations indicated that any quick method of relating γ_j to u_i would lose accuracy but that any accurate method would involve a price in computational speed. Robustness in the solution procedure was preferred to gains in computational speed and so a slow but accurate solution strategy was chosen.

Formally, the choices that need to be made involve the type of vorticity panels used to obtain k_{ij} and the method of relating vorticity to surface velocity.

A panel method, based on a linear variation of vorticity with nodal collocation points, was employed. This is described in ref (2). An additional, compatible panel method was also developed to relate γ_j to u_i. This panel method requires the solution of a system of simultaneous equations for each iteration. Some ten years ago this might have seemed computationally prohibitive, at the time of writing it adds about 30 seconds of microcomputer time to each iteration but in the future, this additional time should be significantly reduced. Robustness gained through the use of this panel method should produce significant savings from time that would otherwise have been wasted in failed attempts with less numerically-robust methods.

LINEARLY-VARYING VORTICITY PANELS

Details of panelisation and the relationship of ψ to γ are given in ref (2). For completeness, a summary of those details is given here, together with full details of the method for relating u_i to γ_j.

For each panel, a local axis system is defined in terms of $\eta - \xi$ coordinates. The panel length is 2c, with nodes 1 and 2 at ξ ordinates of $-c$ and $+c$ respectively. A linear variation of vorticity to either node is described with the aid of the shape functions:

$$N_1 = \tfrac{1}{2}\left(1 - \frac{s}{c}\right) \tag{22}$$

$$N_2 = \tfrac{1}{2}\left(1 + \frac{s}{c}\right) \tag{23}$$

The values of ψ for unit values of vorticity at the ends 1 and 2 of the panel are evaluated for each shape function and expressed in terms of k_{ii}, k_{i1}, k_{21}, k_{12}, k_{22} and k_{i2}. The element k_{ij} is formed by summing the influences at collocation point i of those shape functions having a value of unit at node j. Essential results are summarised in Appendix I.

The problem of relating tangential of relevant vorticity effects over a panel. Relevant integrals are evaluated in Appendix II.

CALCULATION OF NODAL VORTICITY

Non-dimensional surface velocities (U'/Uo or U) are sub-divided into a component due to the free stream and a component due to the effects of the all vorticity panels, i.e.

$$\{U\} = \{\cos(\theta-\alpha) + U_i\} \tag{24}$$

Calculation of $\{U_i\}$ involves integrating the vorticity effects at collocation point i, from all panels. A set of influence coefficients (a_{ij}) is calculated using the results of Appendix II and formed into a matrix [A]. An equation for {U} can then be written:

$$\{U\} = [A]\{\gamma\} \tag{25}$$

This is introduced into equation (24) as

$$\{U\} = \{\cos(\theta-\alpha)\} + [A]\{\gamma\} \tag{26}$$

Rearranging, $\{\gamma\}$ can then be found as:

$$\{\gamma\} = [A]^{-1}\{U - \cos(\theta-\alpha)\} \tag{27}$$

VISCOUS MODEL

The broad outline of the viscous model follows; Hiemenz flow is assumed at a stagnation point, A Thwaite's integration is used to calculate the laminar boundary layer, the Smith-Gamberoni criteria is used to predict transition and the Lag-Entrainment method used for the turbulent boundary layer.

The Hiemenz flow at the leading edge stagnation point is assumed to behave like that around a cylinder of radius 'r'. A nose radius 'r' is computed from aerofoil geometry and the starting conditions for the laminar boundary layer are then:

$$\theta = 0.29234 \sqrt{\frac{\nu r}{2 U_o}} \tag{28}$$

$$\delta_1 = 0.64791 \sqrt{\frac{\nu r}{2 U_o}} \qquad (29)$$

Thwaite's integral between points 1 and 2 can be evaluated (using the assumption of linear velocity variation) as:

$$\theta_2^2 = \left(\frac{U_1}{U_2}\right)^6 \theta_1^2 + \frac{0.45}{6} \nu \cdot \frac{s_2 - s_1}{U_2 - U_1} \left(1 - \left[\frac{U_1}{U_2}\right]^6\right) \qquad (30)$$

Using $$\lambda = \frac{\theta^2}{\nu} \frac{dU}{dx} \qquad (31)$$

and $$H = 2.61 - 3.75\lambda + 5.24\lambda^2 \quad (0 \leqslant \lambda \leqslant 0.1) \qquad (32)$$

$$= 0.0731/(0.14 + \lambda) + 2.088 \quad (-0.1 \leqslant \lambda \leqslant 0) \qquad (33)$$

then $$\delta_1 = H.\theta \qquad (34)$$

(where δ_1 is the displacement thickness, generally rather than at points 1 or 2).

The Smith Gamberoni Transition criteria is quoted in ref (5) as:

$$R\theta_{tr} = 1.174 \left[1 + (22\,400/Rx)\right] Rx^{0.46} \qquad (35)$$

The Lag-Entrainment method is described in ref (6), where equations A-10 to A-32 are arranged in order to facilitate programming. These equations provide the inputs for a momentum integral equation, entrainment equation and lag equation, which are then solved by a Runge-Kutta-Merson initial-value method.

The essential output from the viscous model is the displacement thickness (δ_1), which is used with equation (20) to calculate ψ_i, in preparation for a new estimate of geometry (y_i) from equation (21).

KARMAN TREFFTZ AEROFOILS AND THE TRAILING EDGE CONDITION

The Karman Trefftz analysis for aerofoils with finite trailing edge angles, is described in ref (7). This analysis was employed to provide a yardstick, against which the present method could be tested and to investigate the issue of an

appropriate trailing edge condition. Two candidate methods are described in ref (2) which are:

$$\gamma_1 + \gamma_{n+1} = 0 \qquad (36)$$

$$\gamma_1 - \gamma_{n+1} = 0 \qquad (37)$$

Indices 1 and n+1 refer to γ values on lower and upper surfaces respectively at the trailing edge. Equation (37) was found to be the most appropriate for viscous flow around an aerofoil. One reason for this finding was that equation (36) implies the existence of a rear stagnation point in viscous flow (for which there is no experimental evidence). An additional, important point also became clear while this issue was being investgated.

An examination was made of the distance over which a Karman-Trefftz velocity distribution decayed to zero at the trailing edge. This was found to be very, very small; in fact too small to allow a good representation using the panel method devised, even in inviscid flow. The effects of the vorticity panels depend on $\int\gamma ds$ and so if the length of a panel is insignificantly small then its integrated effects can be ignored. To model vorticity effects at the trailing edge properly, it becomes necessary to prescribe a finite trailing edge velocity which will fair in reasonably with both upper and lower surface velocity distributions. An example of this is shown in Fig 2, where up to the trailing edge a Karman-Trefftz velocity distribution is used and at the trailing edge U/Uo is raised from zero to 0.865.

MESH DETAILS

The majority of panel methods are formulated in terms of geometry and an inflow velocity. This usually results in at least one singularity somewhere on a panel and requires a careful choice of both collocation points and mesh for a successful method. Considerable effort is often needed in mesh 'tuning' and strange answers can be generated when the mesh is changed or used in circumstances for which it has not been tuned. This created an expectation that mesh details would need to be carefully examined before the present method could work.

Examination of the integrals in Appendix I reveals that the relationship between stream function and aerofoil geometry, using nodal collocation points and linearly-varying vorticity panels proves to be non-singular. This should make the

present model less sensitive to the type of mesh used, provided that it permits sufficient panels to represent both an aerofoil's geometry and the vorticity variation that occurs naturally over an aerofoil's surface. Typically, the vorticity distribution varies rapidly near the leading and trailing edges and so panels may need to be concentrated in those regions.

In the mesh employed, the relationship

$$\frac{x}{c} = 0.5\ (1 - \cos\theta) \qquad (0 \leqslant \theta \leqslant \pi) \tag{38}$$

is used to generate panels with an equal increment of θ, so that the required panel concentration occurs at either end of the aerofoil. Another method, described in ref (2) was also used. This concentrates panels in regions of high curvature. Experience with both meshes produced similar answers, supporting the hypothesis that the basic stream function method is not unduly sensitive to the type of mesh used; with the proviso that whatever mesh is used can represent both the geometry of the section and the vorticity variation over its surface.

CORRELATION WITH KARMAN TREFFTZ AEROFOILS

Fig 2 shows a velocity distribution for a Karman Trefftz aerofoil. Clearly, a viscous calculation for the same velocity distribution should produce a profile which is about a displacement thickness inside the inviscid profile. This implies that a cross-over of the upper and lower surfaces will exist at the trailing edge. Unfortunately, cross-overs of vorticity panels produce instabilities in the iteration and so the model needs to be modified for these particular calculations. As a general point, it should be noted that a velocity distribution which is feasible in inviscid flow and produces zero thickness at the trailing edge, will <u>not</u> be feasible in viscous flow since displacement thicknesses produce a cross-over of upper and lower surfaces.

The following modified method was used to investigate the plausibility of Karman-Trefftz velocity distributions in viscous flows:

(i) The location of the displacement surface is given by:

$$y_i + \delta_{1i} \cos \theta i \tag{39}$$

(ii) Introducing (20) into (21) and adding $\delta_{1i} \cos \theta_i$ to both sides produces:

$$y_i + \delta_{1i} \cos\theta_i = \delta_{1i} \left[\cos\theta_i - \frac{U_i}{U_o\ c\ \cos\alpha}\right] +$$

$$\frac{1}{\cos\alpha} \left[x_i \sin\alpha + \sum_j k_{ij}\ \gamma_j\right] \qquad (40)$$

Equation (40) can now be solved iteratively for the displacement surface position ($y_i + \delta_{1i} \cos\theta_i$) and y_i found by subtracting $\delta_{1i} \cos\theta_i$ from the y ordinate of the displacement surface.

Results of an iterative solution to (40) using the velocity distribution shown in Fig 2, are given in Figs 3, 4 and for Reynolds Numbers of 500,000, and 20 x 10^6. As expected, a cross-over of the upper and lower surface profiles does occur, which becomes progressively less pronounced as the Reynolds Number is increased.

The viscous profiles are about a displacement thickness inside the inviscid profiles, indicating that the aerofoil design method is plausible.

DEVELOPMENT OF A PRACTICAL DESIGN METHOD

Equation (40) is a more stable formulation of the aerofoil design problem than (22), as cross-overs in trailing edge vorticity panels are less likely. Observations on the way profiles changed with successive iterations suggested that the use of equation (40) could be improved by the introduction of under-relaxation whenever the two aerofoil surfaces approached eath other at the trailing edge. Defining ω as a relaxation factor, L as a length scale, y_1 and y_{n+1} as the y ordinates of the lower and upper aerofoil surfaces respectively, then:

For $$y_{n+1} - y_1 \geqslant L, \quad \omega = 1 \qquad (41)$$

For $$y_{n+1} - y_1 \leqslant L, \quad \omega = \frac{y_{n+1} - y_1}{L} \qquad (42)$$

If m is the iteration number, then equation (40) is interpreted as:

$$\{y_i + \delta_{1i} \cos\theta_i\}_{m+1} = \{y_i + \delta_{1i} \cos\theta_i\}_m (1 - \omega) +$$

$$\omega \, , \, \{\delta_{1i} \left[\cos\theta_i - \frac{U_i}{U_o \, c \, \cos\alpha}\right] + \frac{1}{\cos\alpha} \left[x_i \sin\alpha + \sum_j k_{ij} \gamma_j\right]\} \qquad (43)$$

Examination of (41) - (43) shows that whenever the two (trailing edge) aerofoil surfaces are more than a distance L apart, any previous geometry is discarded during the iteration cycle. When the two aerofoil surfaces are less than a distance L apart, the credibility given to the newly-computed solution is progressively reduced as the surfaces approach each other. This can be a recipe for blunt trailing edges, but the degree of bluntness may be reduced by using the output of a coarse calculation as the input for a more accurate calculation. Typically, an initial estimate for L is 0.01 (i.e. 1% of chord) and a resulting aerofoil might have a trailing edge thickness of 0.3% chord. This algorithm can also include a trap to avoid negative values of ω, in which case naturally-occurring trailing edge cross-overs need not be inhibited. The Karman-Trefftz velocity distributions examined earlier were re-calculated using the present method and crossed-over trailing edge profiles resulted.

It is necessary to monitor successive iterations to check that geometries are changing slowly, using reasonable value of ω, prior to cessation of the calculation. If this condition is satisfied, then the underlying equations should also be satisfied, as the new geometry is consistent with a correctly-located distribution of vorticity. Should the relaxation factor (ω) become too small, the length scale (L) should be re-defined to raise values of w so that geometry changes can be monitored adequately.

The question of a design incidence appropriate to a velocity distribution tends to be self-evident once a profile is generated. Initially, a design incidence is assumed and the resulting profile is usually inclined at some angle to the x axis. That angle is used as a correction to the initially-assumed incidence and the profile re-computed until the chord line becomes coincident with the x axis.

Surface velocity distributions for feasible aerofoil shapes are difficult to define intuitively without adequate background of shape/velocity distribution relationships for existing aerofoils. In particular, problems can occur at the leading edges. At the present time, the work is used to define an aerofoil profile consistent with a required velocity distribution over its centre and rear chord. Leading edge details may need to be decided by manual fairing. The resulting aerofoil is then evaluated with an analysis program and further modifications made to improve off-design performance. In theory, there is no reason why the method could not be used to produce an accurate initial design of an aerofoil but in practice, until a background of surface velocities/aerofoil-profiles relationships are available, a designer will have difficulty in knowing what information to input to the program.

CONCLUDING COMMENTS

An aerofoil design method suitable for calculating the aerofoil shape consistent with a prescribed EIF velocity distribution has been described. The method does not set out to prescribe the initial EIF surface velocity distribution and the problems associated with doing that have been outlined in the paper.

The iterative procedure described involves a non linear algebraic equation which cannot be guaranteed to converge for an arbitrary velocity distribution when starting from an initially assumed aerofoil shape. Techniques outlined in this paper tend to stabilise that convergence process. Convergence can also be aided through the use of an initial aerofoil profile that has a substantial trailing edge thickness. This tends to allow the bulk of the aerofoil profile to converge before problems with the upper and lower surfaces crossing at the trailing edge begin to appear.

It has been mentioned already that experience with the stream function method suggests it is largely insensitive to the particular mesh used. This quality makes it very suitable for exploring aerofoil profiles corresponding to novel velocity distributions.

Essential innovations of the present work are the inclusion of viscous effects in the aerofoil profile calculation, the development of a panel method to relate surface vorticity to surface velocity, the deployment of vorticity on the displacement surface and a selective introduction of under-relaxation when the iterative process is in danger of diverging. These innovations appear adequate to produce a workable aerofoil design method for viscous flows, but there should be no doubt that a good initial estimate of a surface velocity distribution is a pre-requisite for a

successful aerofoil design. Finally, the method looks easier in theory than it is to implement in practice.

REFERENCES

1. Kennedy, J.L., Marsden, D.J. 'A Potential Flow Design Method for Multicomponent Airfoil Sections'. Journal of Aircraft, Vol. 15, No. 1, January 1978, pp 47–52.

2. Soinne, E., 'Design of Single Component Airfoils Using An Inverse Boundary Element Method' – Helsinki University of Technology Report No. 83–A2 Series A, 1983.

3. Lock, R.C., Williams, B.R. 'Viscous–Inviscid Interactions in External Aerodynamics' – progress in Aerospace Science, Vol. 24, pp 51–171, 1987.

4. Glauret, H. 'Elements of Aerofoil and Airscrew Theory'. Cambridge University Press, 2nd Edition, 1946.

5. Cebici, T., Bradshaw, P. 'Momentum Transfer in Boundary Layers'. McGraw Hill, 1977.

6. Green, J.E., Weeks, D.J., Brooman, J.W.F. 'Prediction of Turbulent Boundary Layers and Wakes in Compressible Flow by a Lag–Entrainment Method'. R&M No. 3791, HMSO, 1977.

7. Milne Thompson 'Theoretical Hydrodynamics'. Fifth Edition, MacMillan Press, 1979, pp198–199.

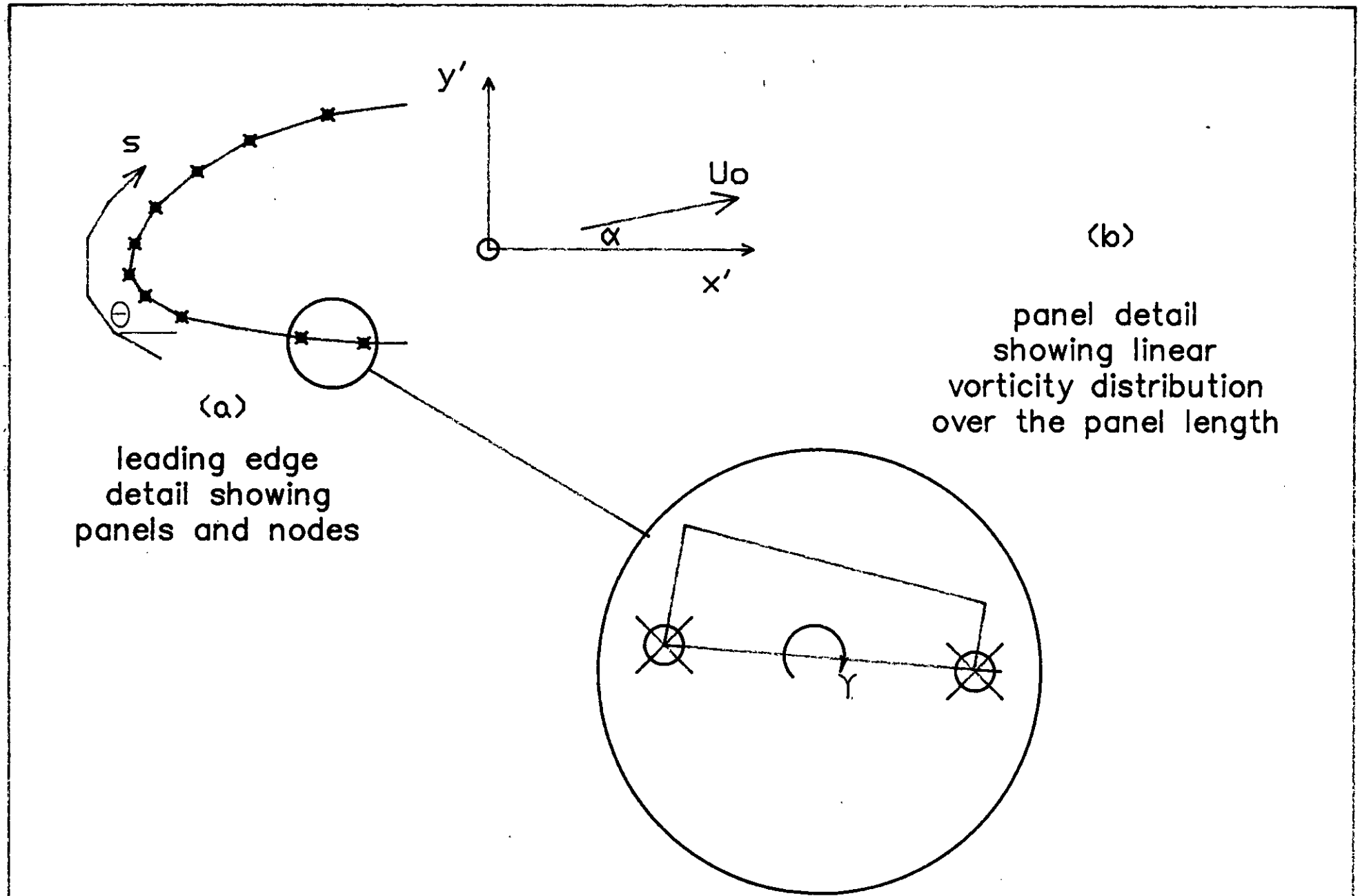

Figs 1(a) & 1b NOTATION AND VORTICITY PANELISATION

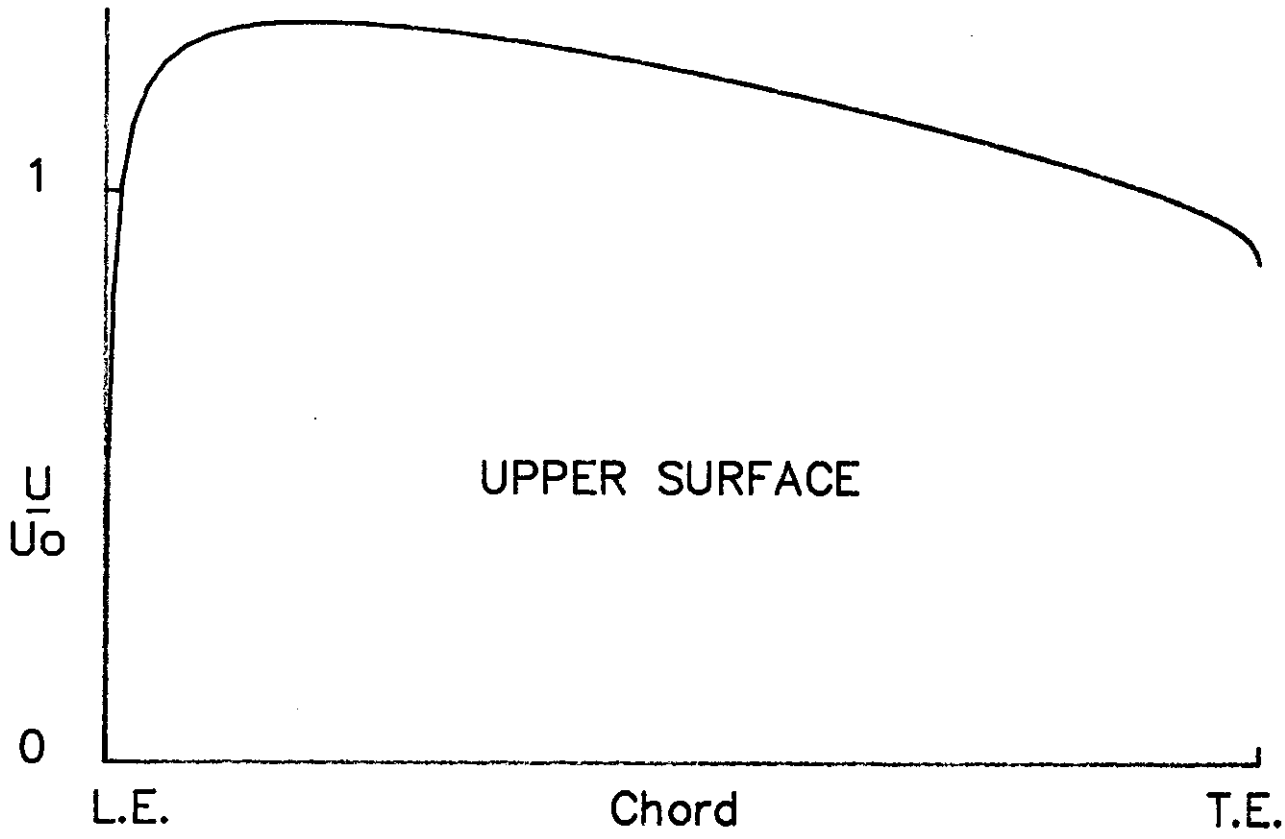

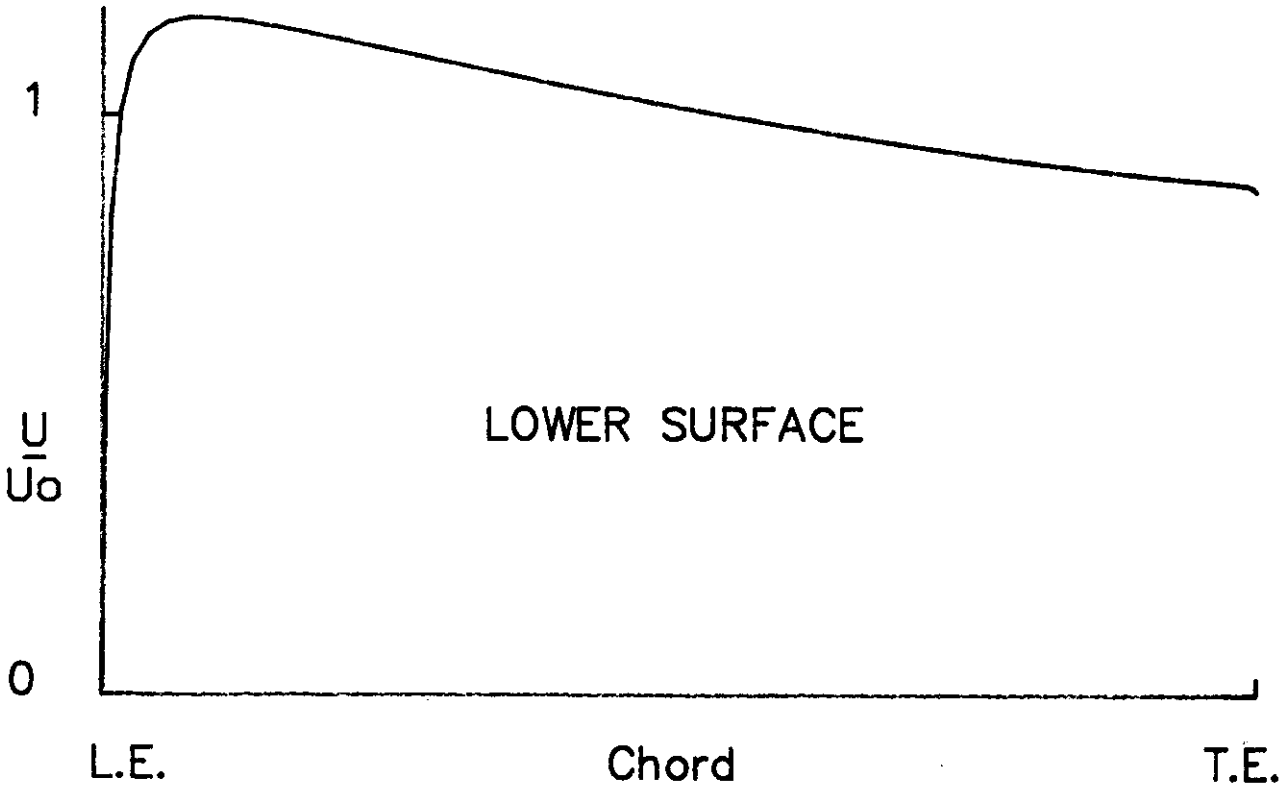

Fig 2 SURFACE VELOCITIES FOR AEROFOILS

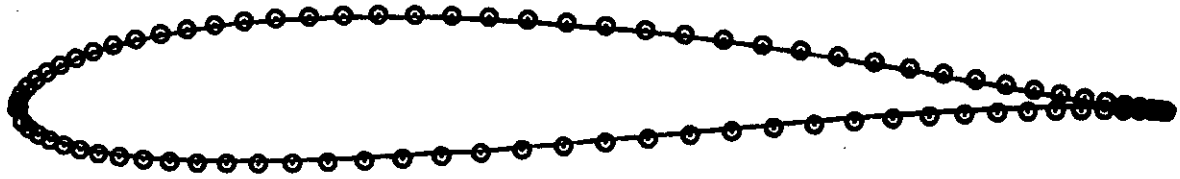

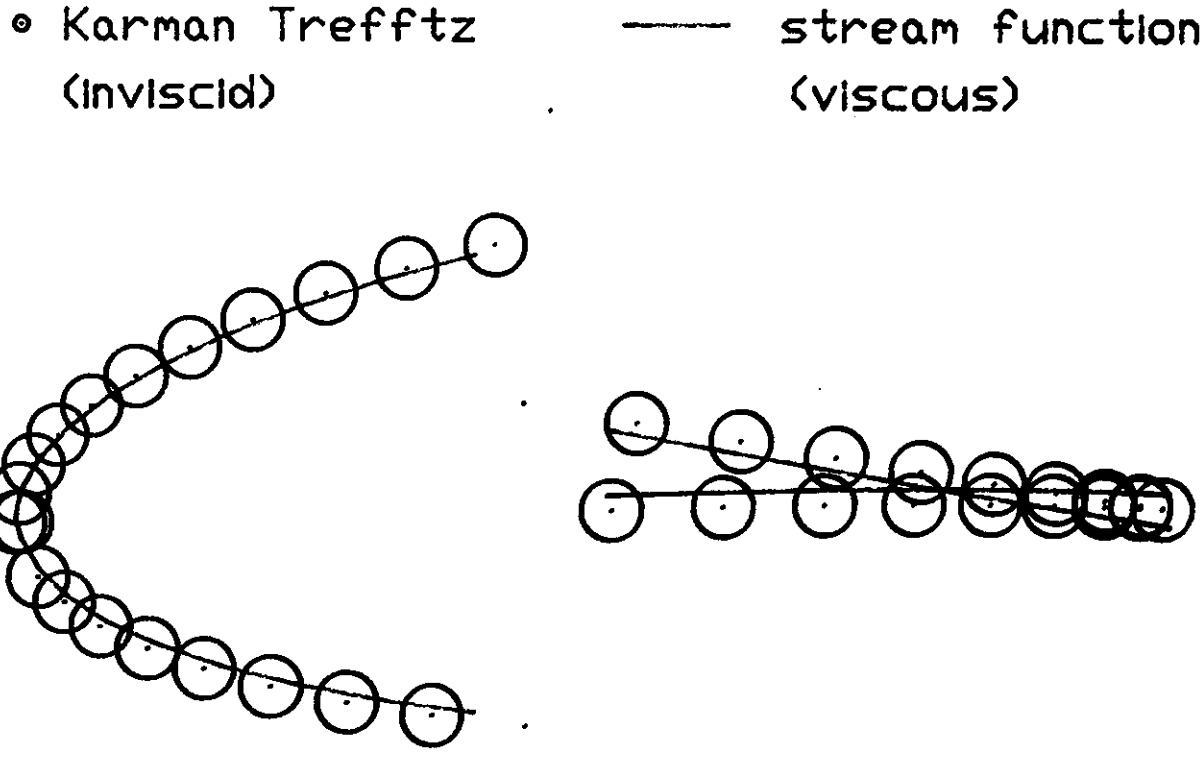

Fig 3 COMPARISON OF VISCOUS AND INVISCID SOLUTIONS, Rn = 500,000.

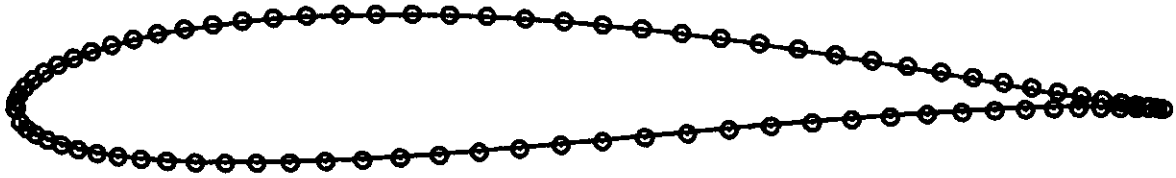

⊙ Karman Trefftz (inviscid)

—— stream function (viscous)

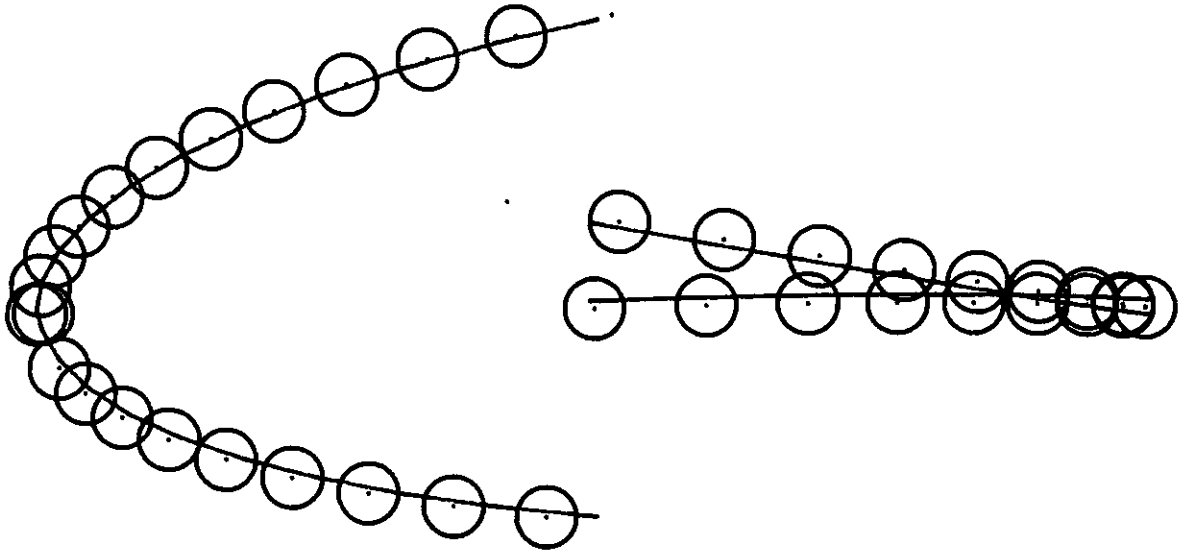

leading edge detail

trailing edge detail

Fig 4 COMPARISON OF VISCOUS AND INVISCID SOLUTIONS, Rn = 20,000,000.

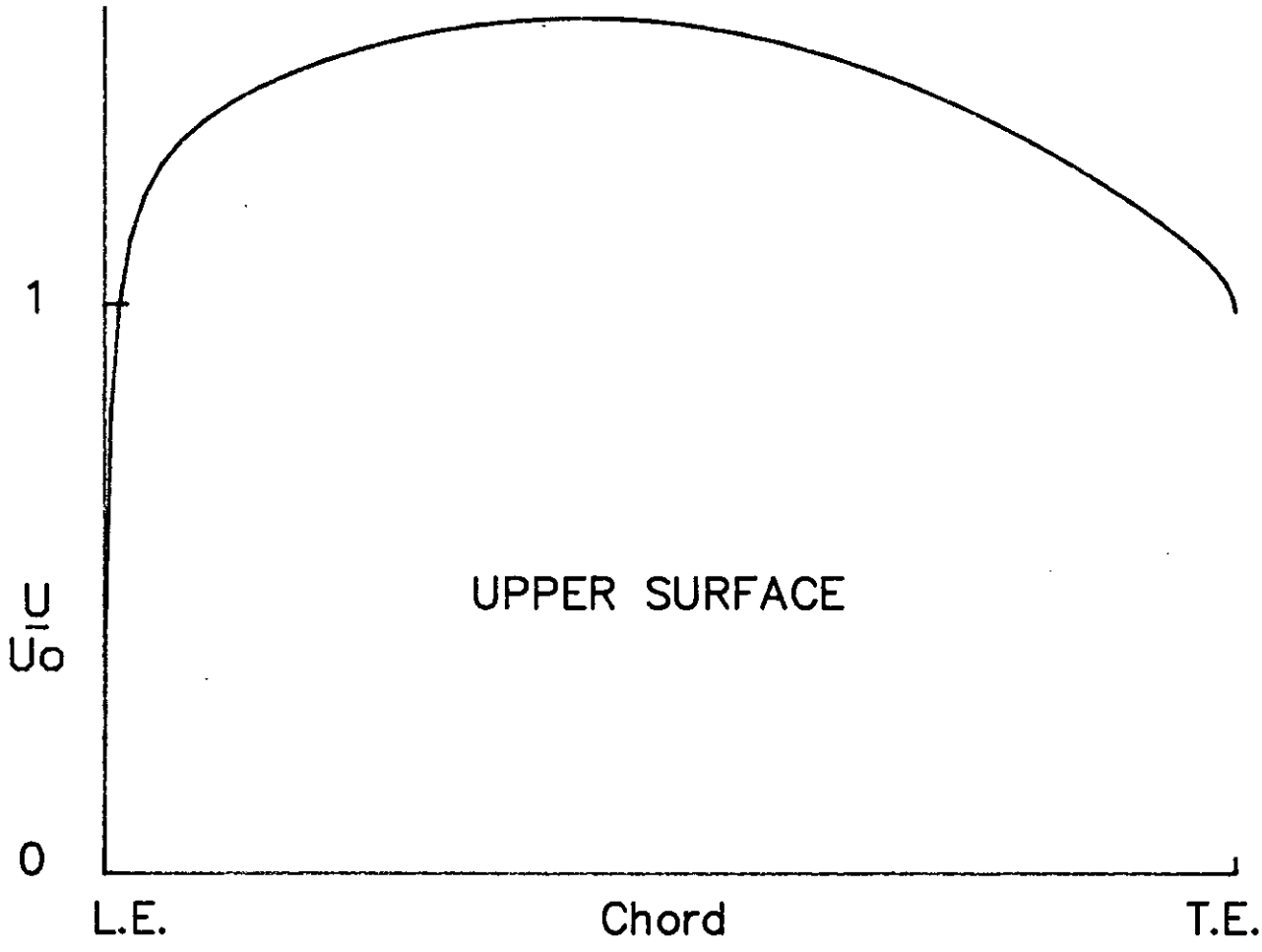

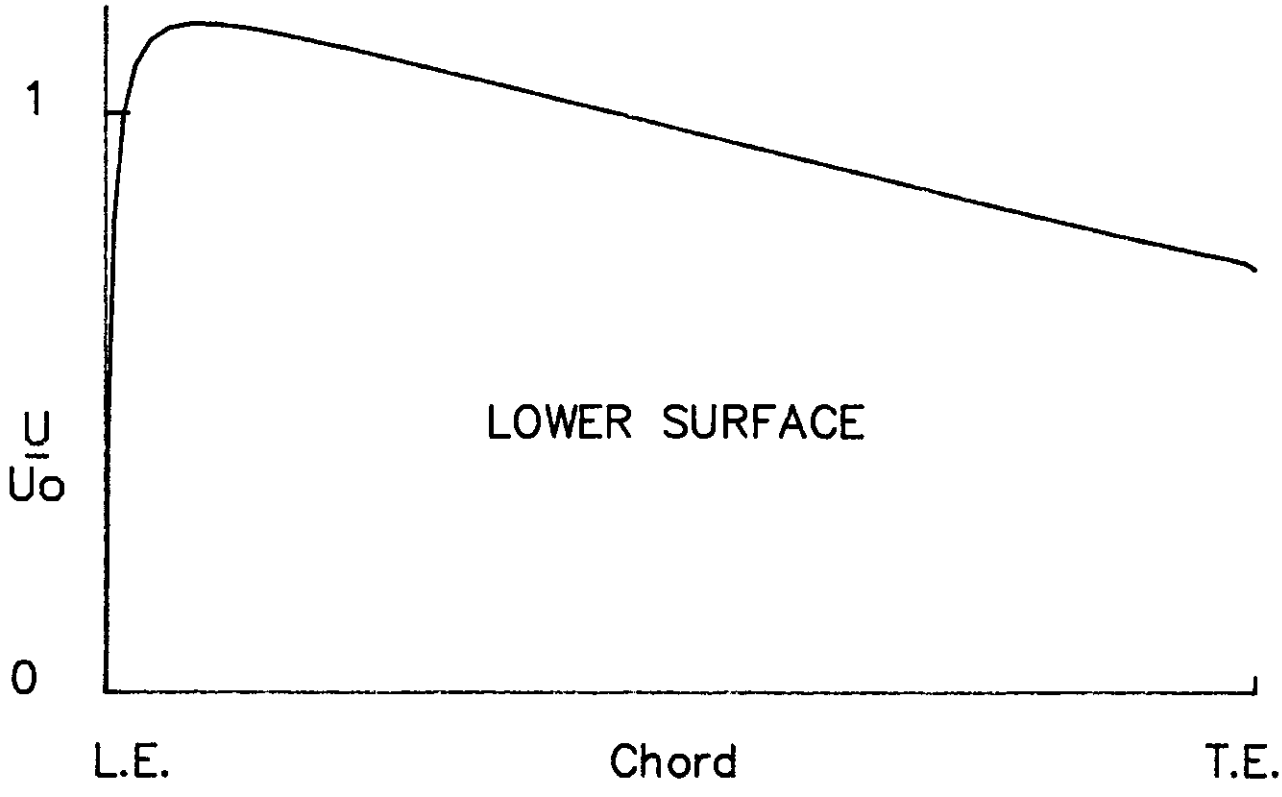

Fig 5 SURFACE VELOCITY FOR AEROFOIL

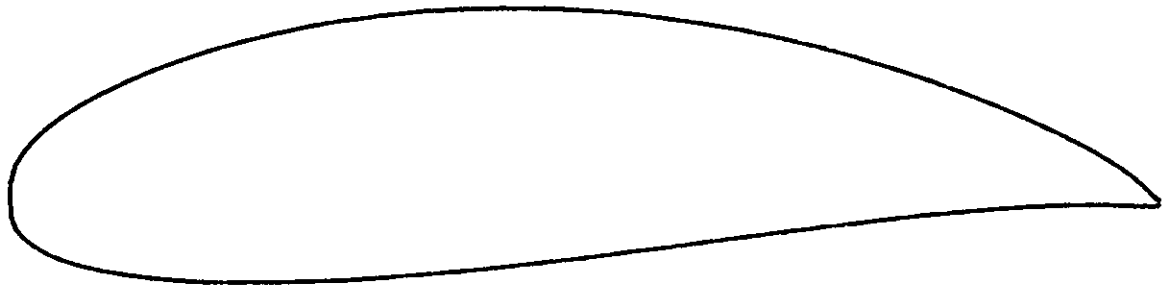

Rn = 2000000; Design Incidence = - 1.1 degrees

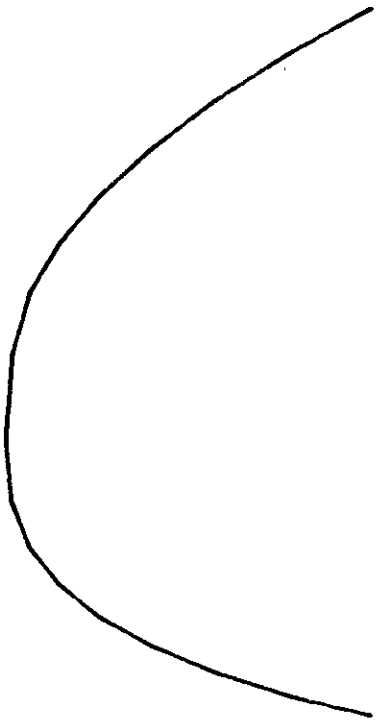

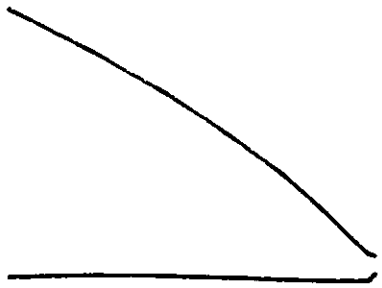

Nose Detail

Tail Detail

Fig 6 VISCOUS FLOW RESULT FOR VELOCITY DISTRIBUTION SHOWN IN Fig

APPENDIX I - STREAM FUNCTION INTEGRALS

The local (ξ,η) coordinate system is shown in Figs A1.1 and A1.2 together with plots of the shape function and other details of panel notation.

The value of ψ_i from a vortex element on a panel is given by:

$$\psi_i = \frac{1}{2\pi} \int_{-c}^{c} \gamma(s) \ln r \, ds \qquad (1)$$

For a complete panel, the integral is:

$$\psi_i = \frac{1}{2\pi} \int_{-c}^{c} (N_1 \gamma_1 + N_2 \gamma_2) \ln r \, ds \qquad (2)$$

The problem now is to evaluate equation (2) for both shape functions N_1 and N_2 to find k_{i1}, k_{i2}, k_{12}, k_{21}, k_{11}, and k_{22}.

From ref (2) these integrals are evaluated as:

$$k_{i1} = -\frac{1}{4\pi}\{(a+c)\ln r_1 - (a-c)\ln r_2 - 2c + b\left[\arctan\frac{a+c}{b} - \arctan\frac{a-c}{b}\right]\} + \frac{1}{4\pi}\{\frac{a^2-b^2-c^2}{2c}\left[\ln r_1 - \ln r_2\right] - a + \frac{ab}{c}\left[\arctan\frac{a+c}{b} - \arctan\frac{a-c}{b}\right]\} \qquad (3)$$

$$k_{i2} = -\frac{1}{4\pi}\{(a+c)\ln r_1 - (a-c)\ln r_2 - 2c + b\left[\arctan\frac{a+c}{b} - \arctan\frac{a-c}{b}\right]\} - \frac{1}{4\pi}\{\frac{a^2-b^2-c^2}{2c}\left[\ln r_1 - \ln r_2\right] - a$$

$$+ \frac{ab}{c}\left[\arctan\frac{a+c}{b} - \arctan\frac{a-c}{b}\right]\Big\} \qquad (4)$$

$$k_{12} = k_{21}$$

$$= \frac{c}{4\pi}\left[1 - 2\ \ln\ |2c|\ \right] \qquad (5)$$

$$k_{11} = k_{22}$$

$$= \frac{c}{4\pi}\left[3 - 2\ \ln\ |2c|\ \right] \qquad (6)$$

Analytical and numerical checks were carried out to confirm that equations (3)–(6) were valid, with a positive conclusion.

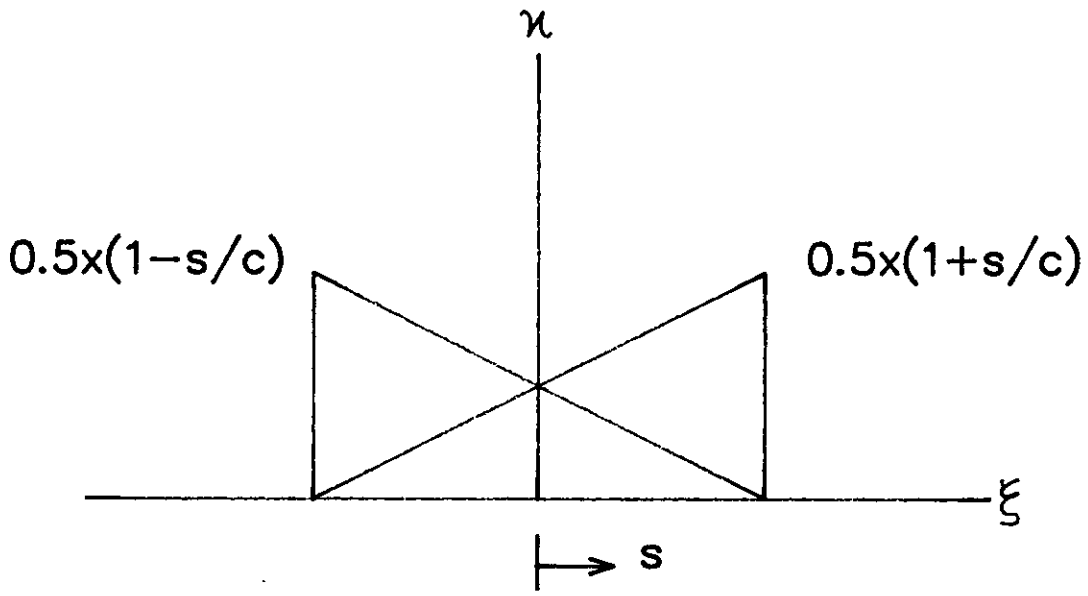

Fig A 1.1 Shape Functions

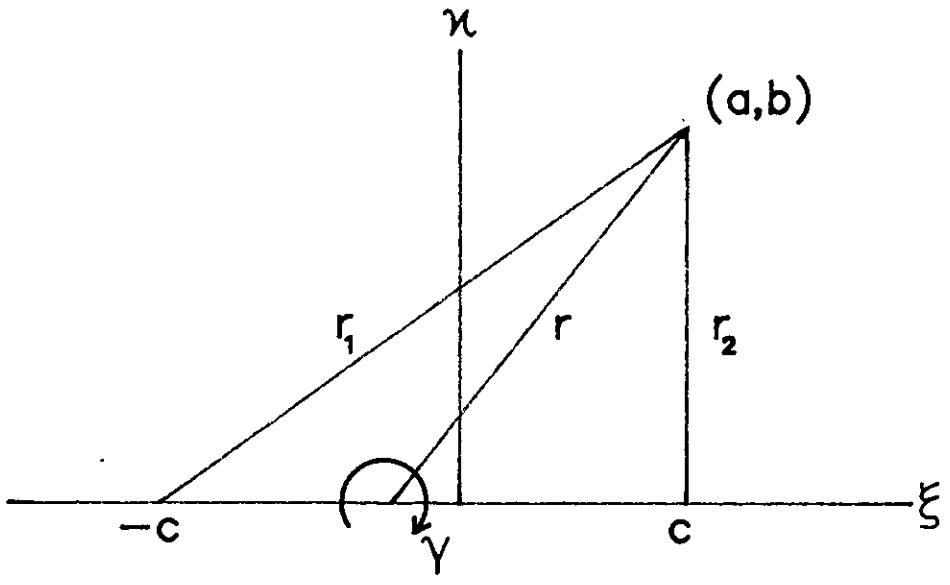

Fig A1.2 Local Coordinates Used For Panel Integrals

APPENDIX II - TANGENTIAL VELOCITY INTEGRALS

The effects of a linearly-varying vortex panel are examined with a view to finding horizontal and vertical (u,v) induced velocity components. Notation is similar to that in Fig A1.1.

Over the panel,

$$\gamma(s) = N_1\gamma_1 + N_2\gamma_2$$

$$= \tfrac{1}{2}\,(1 - s/c)\,\gamma_1 + \tfrac{1}{2}\,(1 + s/c)\,\gamma_2 \qquad (1)$$

Noting that the induced velocity from an element δs is $\gamma\delta s/2\pi r$ with (u,v) components of $\gamma\delta s\ b/2\pi r^2$ and $-\gamma\delta s(a-s)/2\pi r^2$ the integrals to be evaluated are:

$$u = \frac{b}{4\pi}\int_{-c}^{c} \frac{(1-s/c)\,\gamma_1 + (1 + s/c)\,\gamma_2}{(a-s)^2 + b^2}\,ds \qquad (2)$$

$$v = -\frac{1}{4\pi}\int_{-c}^{c} \frac{[(1-s/c)\,\gamma_1 + (1+s/c)\,\gamma_2]\,(a-s)}{(a-s)^2 + b^2}\,ds \qquad (3)$$

Defining,

$$I_1 = \frac{1}{4\pi}\int_{-c}^{c} \frac{ds}{(a-s)^2 + b^2} \qquad (4)$$

and

$$I_2 = \frac{1}{4\pi c}\int_{-c}^{c} \frac{s\,ds}{(a-s)^2 + b^2} \qquad (5)$$

Then (2) can be written

$$u = \gamma_1 \,.\, b\,(I_1 - I_2) + \gamma_2 \,.\, b(I_1 + I_2) \qquad (6)$$

Consequently, calculation of u components to A_{i1} and A_{i2} (analageous to k_{i1} and k_{i2} of Appendix I can be easily carried out once (4) and (5) are evaluated.

By inspection,

$$I_1 = -\frac{1}{4\pi} \int_{-c}^{c} \left[\frac{1}{|b|} \arctan \left(\frac{a-s}{|b|}\right)\right]$$

$$= -\frac{1}{4\pi|b|} \left\{\arctan \left(\frac{a-c}{|b|}\right) - \arctan \left(\frac{a+c}{|b|}\right)\right\} \qquad (7)$$

Noting that $d[(a-s)^2 + b^2]/ds = -2\,(a-s)$, I_2 can be written:

$$I_2 = -\frac{1}{4\pi c} \int_{-c}^{c} \left\{\frac{1}{2} \cdot \frac{-2(a-s)}{(a-s)^2 + b^2} + \frac{a}{(a-s)^2 + b^2}\right\} ds$$

$$= -\frac{1}{4\pi c} \int_{-c}^{c} \frac{1}{2} \cdot \frac{-2(a-s)}{(a-s)^2 + b^2}\, ds - \frac{a}{c} I_1 \qquad (8)$$

I_2 is then evaluated as:

$$I_2 = -\frac{1}{4\pi c} \int_{-c}^{c} \left[\frac{1}{2} \ln |r^2|\right] - \frac{a}{c} \cdot I_1$$

$$= \frac{1}{4\pi c} \left\{-\ln \left|\frac{r_2}{r_1}\right| + \frac{a}{|b|} \left[\arctan \left(\frac{a-c}{|b|}\right) - \arctan \left(\frac{a+c}{|b|}\right)\right]\right\} \qquad (9)$$

Substituting the results from (7) and (9) into (6) gives:

$$u = \gamma_1 \cdot \frac{1}{4\pi c} \left\{-\text{sign}(b)(c-a)\left[\arctan \left(\frac{a-c}{|b|}\right) - \arctan \left(\frac{a+c}{|b|}\right)\right] + b \ln \left|\frac{r_2}{r_1}\right|\right\}$$

$$+ \gamma_2 \cdot \frac{1}{4\pi c} \left\{-\text{sign}(b)(c+a)\left[\arctan \left(\frac{a-c}{|b|}\right) - \arctan \left(\frac{a+c}{|b|}\right) + b \ln \left|\frac{r_2}{r_1}\right|\right\}$$

(10)

Equation (3),

$$v = -\frac{1}{4\pi}\int_{-c}^{c} \frac{[(1-s/c)\ \gamma_1 + (1+s/c)\ \gamma_2]\ (a-s)}{(a-s)^2 + b^2}\ ds$$

is expressed as:

$$v = -\gamma_1\ (I_3 - I_4) - \gamma_2\ (I_3 + I_4) \tag{11}$$

where

$$I_3 = \frac{1}{4\pi}\int_{-c}^{c} \frac{a-s}{(a-s)^2 + b^2}\ ds \tag{12}$$

and

$$I_4 = \frac{1}{4\pi c}\int_{-c}^{c} \frac{s(a-s)}{(a-s)^2 + b^2}\ ds \tag{13}$$

Solving (12)

$$I_3 = \frac{1}{4\pi}\ {}_{-c}^{c}\left[(-\tfrac{1}{2})\ .\ \ln\left|(a-s)^2 + b^2\right|\ \right] \tag{14}$$

$$= -\frac{1}{4\pi}\ln\left|\frac{r_2}{r_1}\right| \tag{15}$$

The integrand in I_4 is rewritten using the relationship:

$$\frac{s(a-s)}{(a-s)^2 + b^2} = -1 + \frac{b^2 + a(a-s)}{(a-s)^2 + b^2} \tag{16}$$

Consequently,

$$I_4 = \frac{1}{4\pi c}\int_{-c}^{c} \left\{-1 + \frac{b^2 + a(a-s)}{(a-s)^2 + b^2}\right\}\ ds \tag{17}$$

Evaluating (16),

$$I_4 = \frac{1}{4\pi c}\ {}_{-c}^{c}\left[-s - |b|\ \arctan\left[\frac{a-s}{|b|}\right] - \frac{a}{2}\ln\left|(a-s)^2 + b^2\right|\right] \tag{18}$$

$$= \frac{1}{4\pi c} \{-2c - |b| (\arctan \left[\frac{a-c}{|b|}\right] - \arctan \left[\frac{a+c}{|b|}\right]) - a \ln \left|\frac{r_2}{r_1}\right|\} \quad (19)$$

Substituting (15) and (19) into (11)

$$v = \frac{\gamma_1}{4\pi c} \{(c-a) \ln \left|\frac{r_2}{r_1}\right| - 2c - |b| (\arctan \left[\frac{a-c}{|b|}\right] - \arctan \left[\frac{a+c}{|b|}\right])\}$$

$$= \frac{\gamma_2}{4\pi c} \{(c+a) \ln \left|\frac{r_2}{r_1}\right| + 2c + |b| (\arctan \left[\frac{a-c}{|b|}\right] - \arctan \left[\frac{a+c}{|b|}\right])\} \quad (20)$$

Pole terms used to be evaluated for u when $a \to \pm c$ and $\eta \to 0$, $x \log x \to 0$ and so the logarithmic terms tend to vanish.

For $s = -c, \quad \eta \to 0$

From 10,

$$u = \frac{\gamma_1}{4\pi c} \{(-2c) [0 - \pi/2]\} \quad (21)$$

$$= \frac{\gamma_1}{4} \quad (22)$$

For $s = c, \quad \eta \to 0$ again from (10)

$$u = \frac{\gamma_2}{4\pi c} \{(-2c) [\frac{\pi}{2} - 0]\} \quad (23)$$

$$u = -\frac{\gamma_2}{4} \quad (24)$$

Transposition of Axes:

There is a problem of converting the induced velocities from a panel orientated at θ_j to the x axis to a tangential velocity (u_T) for a node orientated at θ_i to the x axis. This can be done by transposing the (u, v) velocities through $-\theta_j$ to obtain velocities relative to an (x,y) datum and then through $+\theta_i$ to find the relevant tangential velocity (u_T) i.e.

$$U_T = (u\cos\theta_j - v\sin\theta_j)\cos\theta_i + (u\sin\theta_j + v\cos\theta_j)\sin\theta_i \qquad (25)$$

$$\therefore \quad U_T = u(\cos\theta_j\cos\theta_i + \sin\theta_j\sin\theta_i) + v(\cos\theta_j\sin\theta_i - \sin\theta_j\cos\theta_i) \qquad (26)$$

$$\text{i.e. } U_T = u\cos(\theta_j - \theta_i) + v\sin(\theta_j - \theta_i) \qquad (27)$$

(26) provides the essential equation for calculating coefficients A_{ij} once u and v are known.

SUMMARY

The effects of vorticity at node j on a tangential velocity at node i needs to be computed. For each panel abutting node j, integrals shown in this appendix need to be evaluated to find their contribution to the tangential velocity at node i. Values of γ_1 and γ_2 are set to one or zero as appropriate.

Using panel notation with j = 1, 2; for A_{i1} and A_{i2}, u is found from (10) and (v) from (19). Equation (26) is then used to find the contribution of that panel to A_{ij}.

Where a collocation point coincides with the end of a panel, equations (21) and (23) are used directly to find panel contributions to A_{11} and A_{22}. Values of A_{12} and A_{21} are zero.

Equations (10) and (19) have been checked against numerical integrations of (2) and (3) with good correlation and no obvious doubts about their validity.

CJS(SHIPREP)
15th June 1989

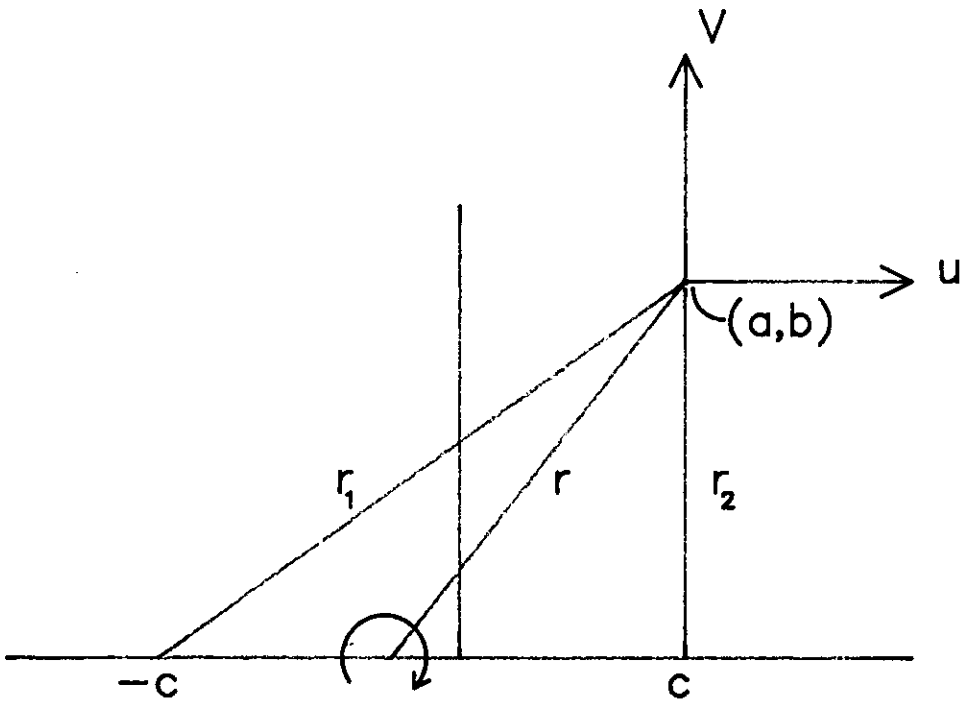

Fig A2.1 Notation for Induced Velocity Integrals